

Seismic bearing capacity of skirted footings using finite element analysis

Rajesh P. Shukla*¹ and Prabir Kumar Basudhar²

¹Department of Civil Engineering, NIT Srinagar, Srinagar, 190006, India

²Department of Civil Engineering, IIT Kanpur, Kanpur, 208016, India

(Received March 20, 2024, Revised August 22, 2024, Accepted August 26, 2024)

Abstract. Studies pertaining to the seismic bearing capacity analysis of skirted footings using the pseudo-static approach for estimation of the earthquake force in association with finite element method have been presented in this paper. An attempt has been made to explain the behaviors of the skirted footings by means of failure patterns obtained for rigid and flexible skirts. The skirts enhance the seismic bearing to some extent with an increase in seismic loading, after which it decreases nonlinearly. The effectiveness of skirts increases initially to some extent with an increase in seismic loading, after which it decreases nonlinearly. Other parameters that inversely affect the effectiveness of skirts are the depth of footing and the internal friction angle of the soil. The detailed finite element analysis regarding the various failure patterns of skirted footings under seismic forces shows the failure mechanism changes from a general shear failure to local shear failure with an increase in seismic force. An opposite trend has been observed with the increase in the angle of internal friction of the soil. The obtained analysis results suggest that a rigid skirted footing behaves similar to a conventional strip footing under seismic and static loadings. The excessive deflection of flexible skirts under combined gravity and seismic loading renders them relatively ineffective than rigid skirts.

Keywords: bearing capacity; improvement factor; seismic loading; skirt; soil; strip footing

1. Introduction

Over the past four decades, various techniques have been developed and evolved to improve the bearing capacity of foundations. Some of the recent studies are due to Azzam and ElWakil (2015), Biswas and Mittal (2017), Demir and Sarici (2017), Al-Aghbari and Mohamedzein (2018), Moradi *et al.* (2019), Shukla and Jakka (2023). Attaching the structural skirt to the footing is one of the techniques that increases the footing depth and improves the overall performance. It enhances bearing capacity and decreases the overall settlement of the foundation (Al-Aghbari and Dutta 2008, Eid 2013, Azzam and ElWakil 2015, Sajjad and Masoud 2018, Shukla 2022). The use of a skirt constrains the soil within it and thereby increases both the footing depth and the bearing capacity (Tani and Craig 1995). Many researches have highlighted the use and benefits of skirted footings under various site conditions, particularly in scenarios where conventional isolated foundations are not advisable, such as in marginal soils, sites prone to scouring, and adverse marine environments (Bransby and Randolph 1999, Hu *et al.* 1999, Al-Aghbari and Mohamedzein 2004, 2006). Additionally, it has also been observed that skirted foundations perform better under inclined loading (Saleh *et al.* 2008, Shukla 2021). The optimal skirt length should equal half the footing's width under inclined loading (Saleh *et al.* 2008).

Randolph and Watson (1999) indicated that failure planes for skirted foundations do not extend to the ground surface, which is in contrast to those associated with conventional strip footings. Al-Aghbari and Mohamedzein (2006) conducted a study that demonstrated that in cohesionless soils, the incorporation of skirts can enhance the bearing capacity of skirted foundations by a factor ranging from 1.5 to 8.1 compared to those for isolated circular footings. Conversely, the contribution of end-bearing resistance to the overall bearing capacity of skirted footings is negligible and may be omitted in the design considerations for such foundations (Yun and Bransby 2007b).

From small-scale model studies on circular skirted footings, Nazir and Azzam (2010) reported a significant increase in bearing capacity when sand piles were utilized in conjunction with skirts. Several other studies have also highlighted the effectiveness of skirted footings in loose soil conditions (ElWakil 2013, Eid 2013, Shukla and Jakka 2022, Bashir *et al.* 2023). Based on numerical modelling, Bienen *et al.* (2012) highlighted that skirted foundations with internal skirts may be economical for large bucket foundations under combined loading. Mana *et al.* (2013) found that a greater number of internal skirts are necessary for circular skirted footings on soils with significant strength heterogeneity. However, this requirement decreases with increasing embedment depth. Mana *et al.* (2014) observed that the displacement of the skirt, influenced by the combined effects of seepage and swelling, ranges from 0.1 to 1 times the diameter of the foundation. Similarly, Stergiou *et al.* (2015) determined that the optimum spacing between skirts under vertical loading is roughly four times the footing diameter. Later, through an experimental

*Corresponding author, Assistant Professor

E-mail: rpshukla@nitsri.ac.in

^aPh.D., Retired Professor

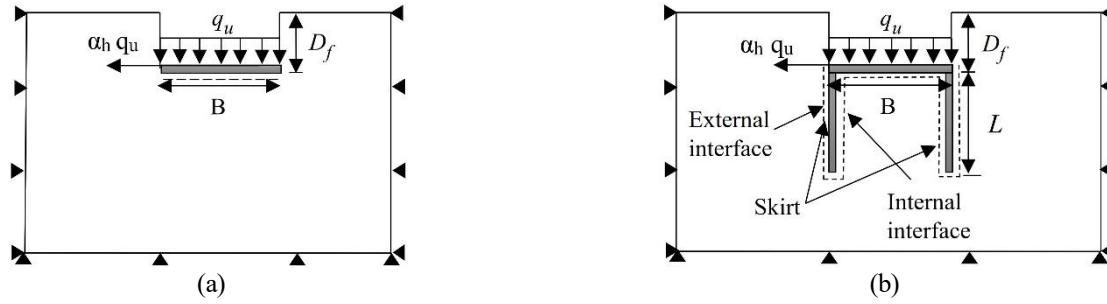


Fig. 1 Typical footings: (a) Strip footing and (b) Skirted footing

investigation, Khatri *et al.* (2017) observed an improvement in the pressure-settlement behaviour of isolated skirted footings resting on the sand. The skirt length and spatial variability of the soil shear strength significantly affect the bearing capacity and failure envelopes (Selmi *et al.* 2019). Yan *et al.* (2020) presented the results of the large-scale model test conducted on a newly designed caisson foundation in sand consisting of two skirted side semicircles and a skirted middle rectangle. It was observed that the foundation sinks due to self-weight and fails due to tilting. Shukla and Jakka (2023) observed that the inclined skirt can further enhance the bearing capacity significantly.

Literature reviews indicate that providing a skirt reduces the settlement significantly and enhances the bearing capacity, primarily due to increased foundation depth. However, there is an ambiguity over the magnitude of bearing capacity enhancement. A number of studies suggested that increasing the conventional strip footings depth is more beneficial than increasing skirt length (Tani and Craig 1995, Yun and Bransby 2007a, Bransby and Yun 2009, Eid 2013, Mana *et al.* 2013, Vulpe 2015). However, some studies show that providing skirts is a better alternative than increasing the depth of conventional isolated footings (Chetia and Das 2010, Al-Aghbari and Mohamedzein 2004, Zhang and Ding 2011). It is noted from literature reviews that earlier studies have not included seismic loading in the analysis, and most studies are focused on circular and rectangular footings under static loading conditions. However, in-depth studies were not made with regard to the seismic performance of these footings. Strip footings are frequently used in most semi-urban and urban areas. Consequently, it is crucial to evaluate the effect of incorporating skirts on the failure mechanism and bearing capacity enhancement of strip footings under seismic loading. There exists a gap in the knowledge in this direction, and further research is essential to close the gap. As such, this study makes an effort to analyze the seismic performance of rigid skirted footings using the finite element method and report the findings with regard to the developed failure mechanism and the corresponding ultimate bearing capacity.

2. Problem statement & analysis

2.1 Problem statement

Typical footings, e.g., a strip footing and a skirted strip footing, are shown respectively in Figs. 1(a) and 1(b)

subjected to forces as shown. As reported in the literature, possible failure mechanisms for these footings are also shown in these Figures. It intends to study the failure mechanism of rigid skirted footings, check the correctness of the conceived ideas, and predict the corresponding ultimate bearing capacity incorporating the seismic on the soil as well as the foundation.

2.2 Assumptions

The following assumptions are made in the analysis: (i) Soil medium is semi-infinite, homogeneous, isotropic, and linearly elastic-plastic. (ii) Plane strain condition exists. (iii) Soil obeys Mohr-Coulomb's failure criterion. (iv) Footing is rigid. (v) The Skirt is made up of a steel plate of negligible thickness. (vi) The connection of the skirt with the rigid foundation is rigid.

The assumptions (i and ii) and (iv, v and vi) do not allow the model to be very precise, but they are practical for many engineering analyses and help to develop models that are both useful and computationally feasible. Bishop (1966) has demonstrated that when the effect of intermediate principal stress is not considered in the failure criterion, assumption (iii) provides results that are reasonable over the whole range of intermediate principal stress representing compression (during loading) and extension (during unloading).

2.3 Numerical modeling

The finite element program Optum G2 has been employed in the analysis. Based on the earlier studies, the domain area of the model has been chosen to be sufficiently large to mitigate boundary effects (Shukla and Jakka 2023). The minimum length (Y-axis) and width (along X-axis) have been chosen to be $30B$ and $15B$, respectively. The horizontal displacement is restrained along the vertical boundaries, while all displacements are restrained along the horizontal (bottom) boundary. The mesh used in the numerical model is depicted in Fig. 2.

The cohesionless soil medium is idealized as a linearly elastic semi-infinite elastic-plastic half-space obeying the Mohr-Coulomb (MC) failure criterion and is divided into a number of 15-noded triangular Gaussian elements. The details of the Mohr-Coulomb model are provided in the Lemaitre, J. (Ed.). Assumptions regarding the structural elements, e.g., the footing and the skirts, are as described above. For simulation, the footing is considered to be a rigid

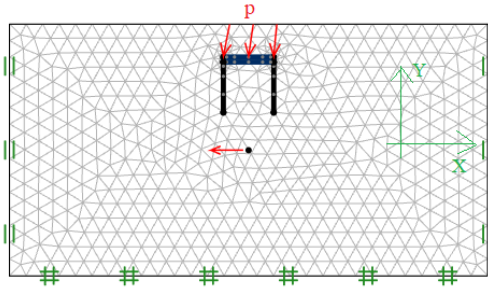
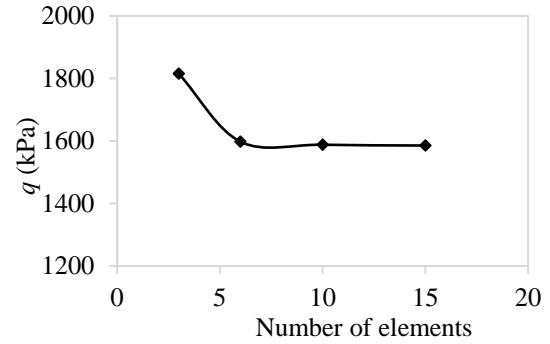


Fig. 2 Typical loaded skirted foundation and adopted mesh for finite element simulation

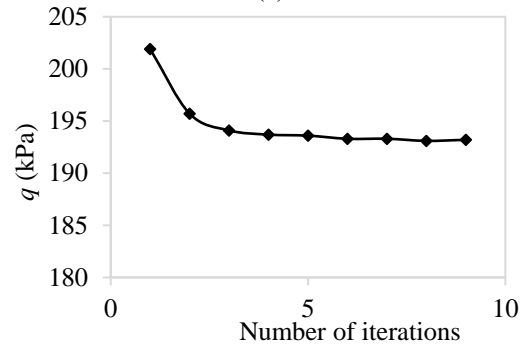
plate, and so is the skirts as plate-like elements. As such, the stiffness of the footing is considered to be infinite in the analysis. The assumption of rigid connections to connect the skirt with the foundation allows the foundation to efficiently transfer the loads from the bottom foundation plate to the skirt and finally transfer the load to the soil. Earlier studies on skirted footings have indicated negligible separation at the inner interface between the skirt and the soil (Chen and Randolph 2007, Mana *et al.* 2012). However, it is likely that the soil will be confined in between the footing and the attached skirt and will have little scope to deform and would possibly act as a single unit; as such, in the present analysis, the inner interface (soil-footing and soil-skirt) has been considered to be highly bonded with the contained soil, allowing no slip; therefore, the value of the interface factor is considered to be unity. However, the value varied from 0.5 to 1.0 for the external interface in the analysis. Values of the interface factor for perfectly rough (bonded) and smooth surfaces are 1 and 0, respectively.

Similar to previous studies, adaptive mesh was used to refine the mesh to obtain accurate results (Lyamin *et al.* 2005, Keawsawasvong and Ukritchon 2016, Shukla and Jakka 2023). One of the most important aspects of the analysis is adaptive iterations, which automatically refine the mesh and save time. Three adaptive iterations were used to refine the mesh in the particular areas (where shear dissipates) without refining the whole domain. The 5 iterations have been used to refine the mesh. It was also found that using more than 9,000 elements does not significantly enhance the results. Consequently, 9,000 elements were utilized in the initial adaptive iterations, which were finally increased to 12,000 in the fifth adaptive iteration. The typical effect of the number of elements and the number of iterations on results (bearing capacity and load intensity q) is shown in Fig. 3. The analysis details can be found in a number of books and earlier published research (Chen and Liu 1990, Sloan 2013, Keawsawasvong and Ukritchon 2017). Therefore, it has not been included herein.

The improvement in the bearing capacity is determined in terms of improvement factors (I_f) and bearing capacity factors ($N_{\gamma q}$). Improvement factor (I_f), indicating the effectiveness of the skirt, is defined as the ratio of the bearing capacity of a skirted footing to that of a conventional strip footing capacity without any skirt. Many factors affect the behaviour of skirted foundations. These



(a)



(b)

Fig. 3 Modelling details: (a) Number of elements and (b) Number of iterations

are the skirt length, soil type, skirt stiffness, soil strength, and depth ratio of footing.

$$I_f = \frac{\text{Bearing capacity of skirted footing}}{\text{Bearing capacity of conventional strip footing}} \quad (1)$$

Parametric studies are made varying those parameters in the analysis as follows:

The angle of internal friction (ϕ): 25° to 45° at an interval of 5° .

The ratio of skirt length (L) and footing width (B): 0 to 2 at an interval of 0.5.

Depth ratio (D_f/B): 0 to 1.5 with a constant interval of 0.5

Horizontal earthquake acceleration (α_h): 0 to 0.3 at an interval of 0.1

Unit weight of cohesionless soil (γ): 15 kN/m³ to 18 kN/m³

The range of these parameters has been selected based on the literature study (Al-Aghbari and Mohamedzein 2004, Yun and Bransby 2007, Eid 2013, Huynh *et al.* 2022, Mase *et al.* 2023).

3. Results and discussions

Using the presently developed approach, results are obtained and discussed below under different subsections.

3.1 Verification of the numerical model

Before proceeding with any detailed analysis of the skirted footing under seismic loading using the developed

Table 1 Comparison of bearing capacity factor (N_γ) with earlier studies

Studies	Method	Constitutive modelling	$\phi=25^\circ$	$\phi=30^\circ$	$\phi=35^\circ$	$\phi=40^\circ$	$\phi=45^\circ$
Present Study	Finite elements	MC	6.78	14.70	35.88	88.71	233.08
Kumar (2003)	Lower Bound FEM	MC	6.46	14.68	34.31	85.10	232.64
Ukritchon <i>et al.</i> (2003)	Upper and lower bound FEM	MC	5.95	13.20	29.30	69.90	165.00
Martin (2005)	Method of characteristics	MC	7.36	16.73	39.18	97.01	260.20
Kumar and Khatri (2008)	Lower bound finite elements	MC	6.02	13.65	31.90	77.88	204.53
Chakraborty and Kumar (2013)	Lower bound finite FEM	MC	6.43	14.53	33.54	81.80	210.00
Zhu (2000)	Upper bound limit analysis		7.86	17.57	40.20	97.92	263.74
Michalowski (1997)	Upper bound limit analysis	MC	9.76	21.39	48.68	118.82	322.83

Table 2 Comparison of numerical results (N_q) with earlier studies

Studies	Method	Constitutive modelling	$\phi=25^\circ$	$\phi=30^\circ$	$\phi=35^\circ$	$\phi=40^\circ$	$\phi=45^\circ$
Present study	Finite elements	MC	15.36	24.34	44.69	90.96	197.92
Yin <i>et al.</i> (2001)	Finite-difference	MC	12.00	22.00	44.00	70.00	180.00
Meyerhof (1965)	Limit equilibrium	MC	10.70	18.40	34.78	64.10	134.70
Terzaghi (1943)	Limit equilibrium	MC	12.65	22.50	41.40	81.30	173.30

model, it is essential to verify the same by comparing the computed results with those of earlier studies available in the literature (Michalowski 1997, Zhu 2000, Ukritchon *et al.* 2003, Kumar 2003, Martin 2005, Kumar and Khatri 2008, Chakraborty and Kumar 2013). Tables 1 and 2 present a comparison of the predicted values of bearing capacity factors by different investigators when the angle of internal friction of soil varies within the range as follows: $45^\circ \geq \phi \geq 20^\circ$. The bearing capacity factors, N_γ , and N_q (the bearing capacity factors related to surcharge and soil unit weight) computed using the present approach are for a rigid strip footing with a rough base resting on cohesionless soils.

The comparison (Table 1) shows that the model used in the present study gives reasonable values of the bearing capacity factor (N_γ), which are closer to those presented by Kumar (2003) but lower than the upper bound solution of Michalowski (1997), Zhu (2002), and the solution by the method of stress characteristics presented by Martin (2005). But it is to be noted that these values are greater than the lower bound solutions as reported by Ukritchon *et al.* (2003), Lyamin *et al.* (2007), Kumar and Khatri (2008), and Chakraborty and Kumar (2013). Table 2 presents a comparative study of N_q values as obtained from the present study with the earlier results. It is evident that the average values align more closely with those reported by Yin *et al.* (2001) using FLAC. However, these values are relatively higher than the bearing capacity, as determined by traditional theories of bearing capacity (Terzaghi 1943, Meyerhof 1965). The differences in the values highlight the limitations of earlier traditional approaches, which treat surcharge loading/overburden as uniformly distributed loading while neglecting the shearing resistance of the soil placed above the footing base. Consequently, earlier studies by Terzaghi (1943) and Meyerhof (1965) yield more conservative estimates of the bearing capacity factor (N_q). Fig. 4 shows that the values of the improvement factor I_f as

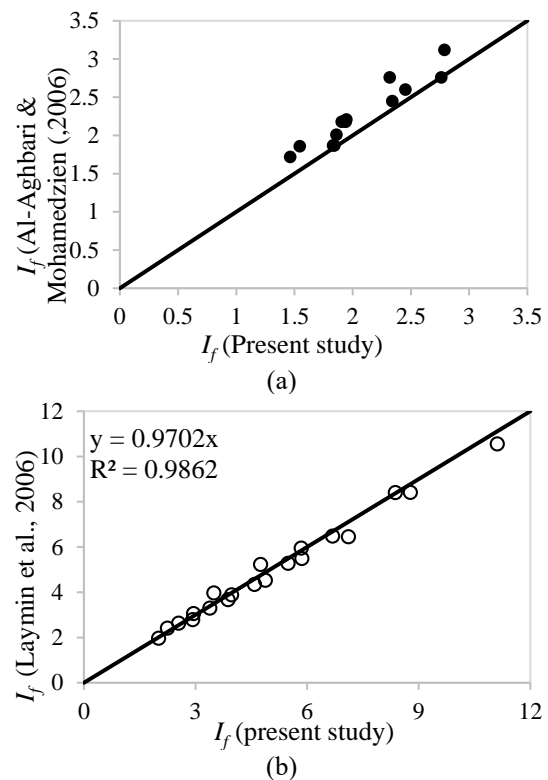


Fig. 4 The comparison of results with published studies for: (a) Deformable skirted (b) Rigid skirt

computed, are comparable to Al-Aghbari and Mohamedzein (2004). The results as obtained in the present study are from numerical modeling of a full-scale problem. However, Al-Aghbari and Mohamedzein (2004) performed a small-scale experimental study to analyze the skirted footing. The computed induced stresses as obtained from small-scale models, are observed to be relatively low. Eid (2013) and Shukla and Jakka (2023) found that the skirts are more

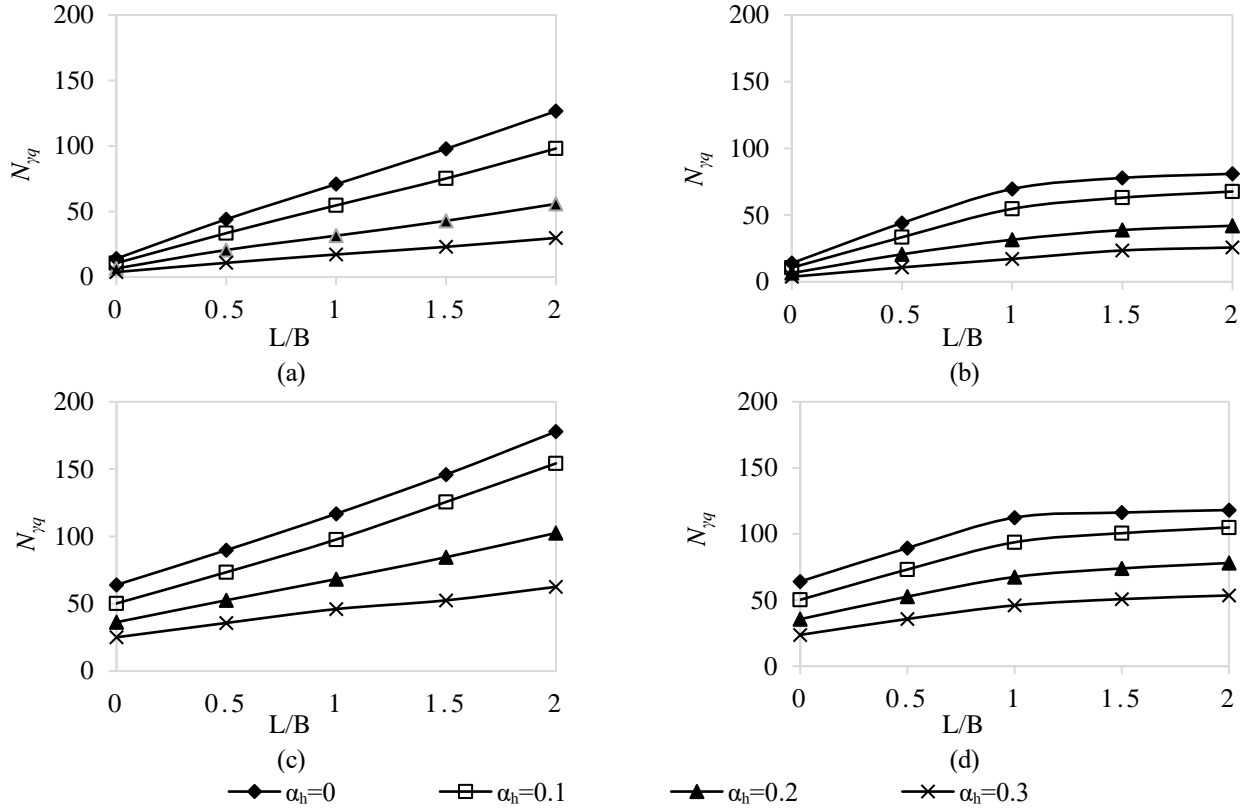


Fig. 5 Variation in $N_{\gamma q}$ with skirt length (a) Rigid, $D_f/B=0$, (b) Deformable, $D_f/B=0$, (c) Rigid, $D_f/B=1.0$ and (d) Deformable, $D_f/B=1.0$

beneficial in loose soils, and efficiency decreases with the soil strength and stiffness. Therefore, experimental I_f is greater in the experimental study than the present full-scale numerical modelling (Fig 4(a)). The coefficient of determination (R^2) value is 0.90 when compared with those reported by Al-Aghbari and Mohamedzein (2004). Scaling effects have also contributed to the differences between the numerical and experimental studies.

Fig. 4 shows the effect of the depth factor for rigid skirt footings, and when compared with those reported by Lyamin *et al.* (2006), the values are found to be in very good agreement. The results from the present study and that of Laymin *et al.* (2006) were obtained by using finite element analysis. Thus, it may be construed that rigid skirted footings behave like solidly embedded strip footings with soil encapsulated and constrained between the two skirts at the edges. The same benefits can be attained in rigid skirted footings, which can be achieved by increasing the depth of the strip footing. Thus, from the results presented in Tables 1 and 2 and Fig. 4, it can be inferred that the numerical model used in this study gives reasonably correct predictive values, which are close to the earlier published results and can be adopted for such problems with confidence. However, these more theoretically sound results need to be validated by comparing with experimental observations for full and final acceptance. From the experience of successful applications and very good predictions using such analysis to several problems with complicated geometry and complex soil behaviour, it can be inferred that with proper modelling of the geometry of the

structure, soil strata, and materials, these can be used for simulating such problems and use the same for practical purposes.

3.2 Performance of skirted foundations: Parametric study

The rigid and deformable skirted footings are analyzed separately. Parametric studies have been conducted varying the skirt length. The behaviours of deformable and rigid skirts are explained by means of the failure mechanism obtained as an outcome of the present analysis.

3.2.1 Effect of skirt length

Figs. 5 and 6 show relationships of seismic bearing capacity factor ($N_{\gamma q}$) for skirted footing and improvement factor (I_f) with the length ratio (L/B) for skirted footings with both rigid and deformable skirts. Figs. 5(a) and 5(c) show for rigid skirts that as the ratio (L/B) increases, the bearing capacity factor ($N_{\gamma q}$) values increase at a constant rate. But from Figs. 5(b) and 5(d), it is observed that as (L/B) increases, there is an increase in the seismic bearing capacity factor. The bearing capacity factor increases up to the length ratio, which is equal to unity, but beyond that, the increase is at a much-decreased rate. Bearing capacity increases with the increasing length of deformable and rigid skirts. The seismic bearing capacity factor of skirted footing increases due to an effective increase in footing depth, an observation similar to other earlier investigators (Tani and

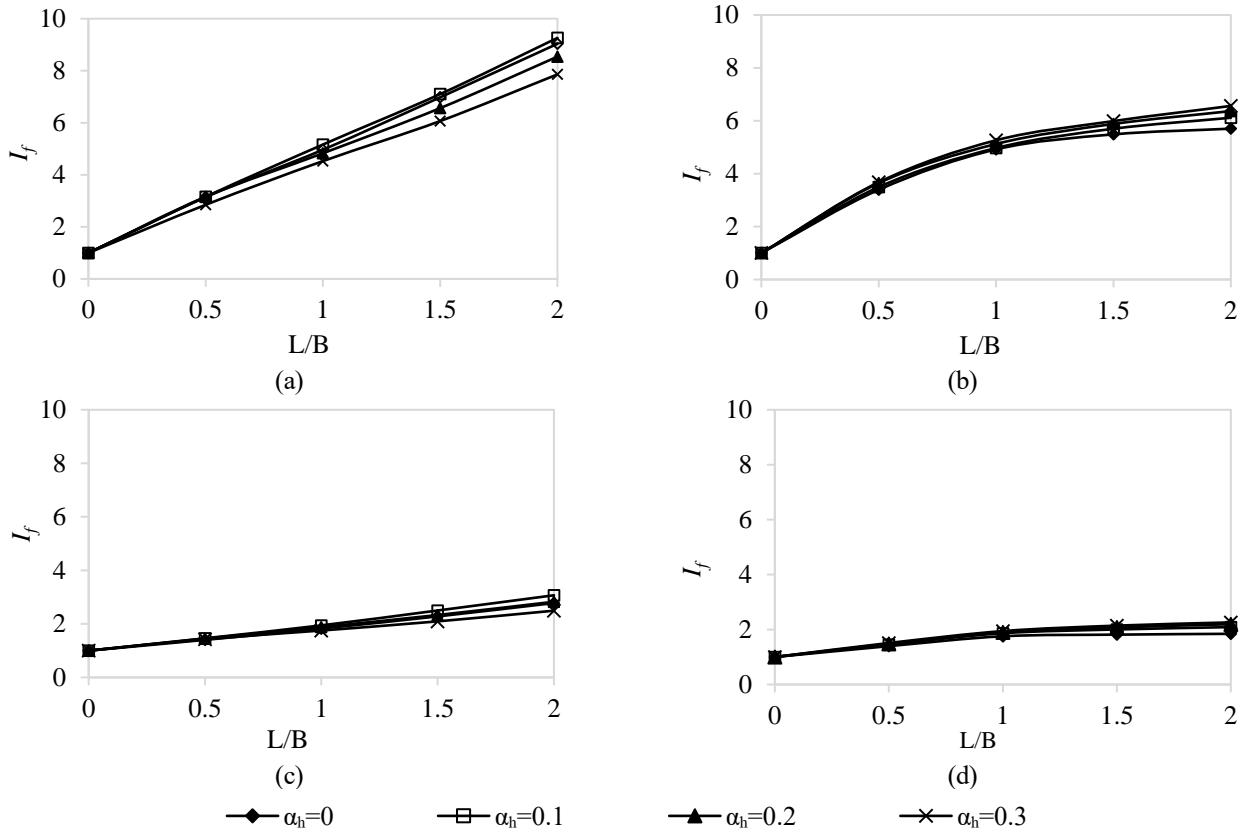


Fig. 6 Variation of improvement factor: (a) Rigid, $D_f/B = 0$, (b) Deformable, $D_f/B = 0$, (c) Rigid, $D_f/B = 1.0$ and (d) Deformable, $D_f/B = 1.0$

Craig 1995, Mase *et al.* 2022). However, the bearing capacity factor initially increases linearly at a constant rate for the deformable skirt. Still, when the (L/B) ratio is greater than unity, the bearing capacity factor increases at a decreased rate, as indicated by the much-decreased value of the relationship curve beyond this point. Similar behaviour is observed in Figs. 6(a) and 6(e) (for bearing capacity factor) and Figs. 6(b) and 6(d) (for improvement factor). It is evident from Fig. 6 that the improvement is not as appreciable for deformable skirts in comparison to those for rigid skirts. The strength of the bearing capacity factor with skirt length is maximal in the footing resting on the ground surface under static loading. However, the influence of the skirt on bearing capacity decreases with increased seismic loading and footing depth (Figs. 5 and 6). It is also apparent that the effect of increasing earthquake acceleration on the values of the bearing capacity factor is very appreciable.

The percentage change in the seismic bearing capacity factor of skirted footing relative to strip footing is presented in Fig 7. The change in bearing capacity factor is significant for the footing resting on the ground surface compared to footing located at some depth below the ground surface. Similarly, the improvement is more significant in rigid skirted footing than flexible footings.

Figs. 8(a) to 8e show typical variations of shear zones developed in cohesionless soil (whose angle of internal friction is 35°) lying beneath the skirts. The shear zones developed in the rigid and deformable skirts are shown in

the left and right parts of each Figure. The shear zone area enlarges with increased skirt length, resulting in an enhancement of the footing bearing capacity. Up to a skirt length of $0.5B$, the shear zone area is symmetrical and identical for both rigid and flexible skirted footings, and the I_f is also almost identical for both footings (Fig. 6). An elastic wedge develops below the rigid strip footing and skirted footings for all the cases, and failure mechanism changes from general to confined failure mode with an increase in length. The deformable skirts with higher lengths deflect toward the direction of soil movement, and the footing behaves like traditional strip footings (highlighted in red in Figs. 8(c), 8(d), 8(e)).

It significantly reduces the effectiveness of the deformable skirt. It leads to the development of a slip surface from the soil confined between skirts. It also originates from the corners of the footing (connection points between skirt and footing) for a higher length of skirts ($L/B > 1$), and as such, its behaviour is identical to that of a strip footing. However, for rigid skirt foundations, the slip line always originates from the tip of the rigid skirt. The shear zone area and length of slip lines are also relatively large in the rigid skirt. The difference in the failure mechanism of deformable and rigid skirts becomes more perceptible with an increase in the skirt length, which leads to a significant difference in the effectiveness of rigid and deformable skirts. The length (L/B) up to which both deformable and rigid skirts behave identically is higher in the static case than in the seismic case. This length is $1B$ for

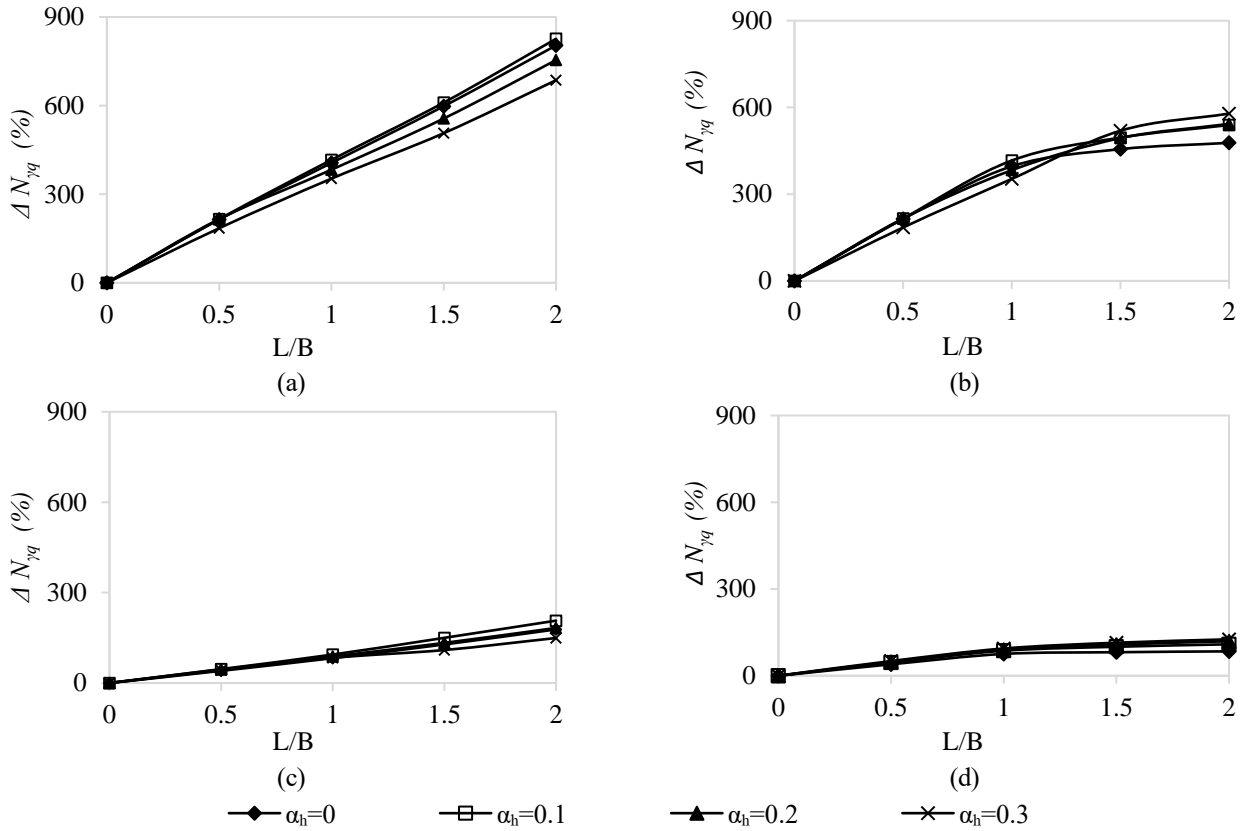


Fig. 7 Percentage change in bearing capacity factor: (a) Rigid, $D_f/B = 0$, (b) Deformable, $D_f/B = 0$, (c) Rigid, $D_f/B = 1.0$ and (d) Deformable, $D_f/B = 1.0$

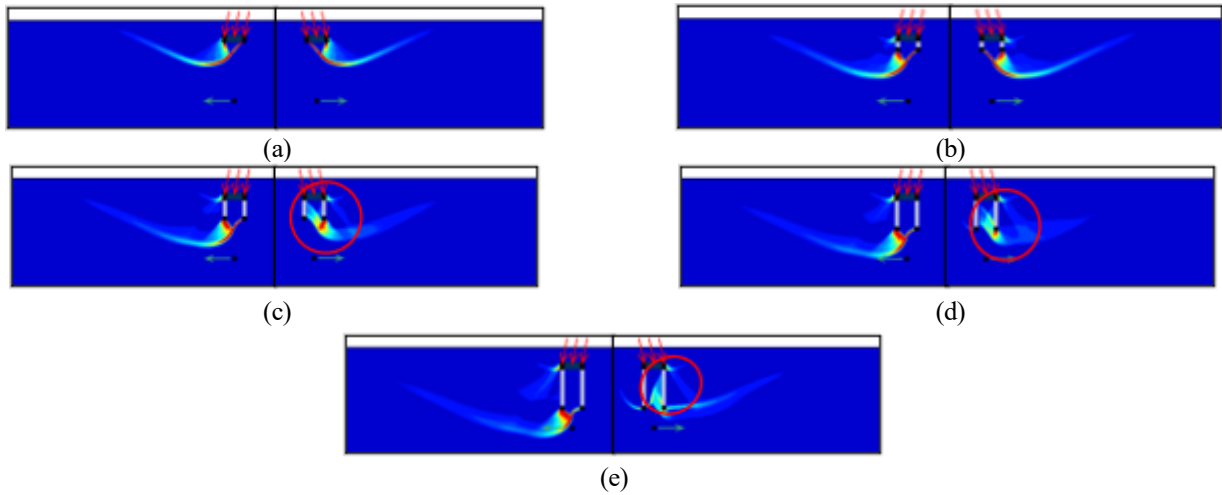


Fig. 8 The variation in failure mechanism with skirt length: (a) $L/B=0$, (b) $L/B=0.5$, (c) $L/B=1.0$, (d) $L/B=1.5$ and (e) $L/B=2.0$

soil with an internal friction angle of 35° under the static case. The deformable and rigid skirts for skirt lengths greater than $0.5B$ behave differently. Mana *et al.* (2012) presented the failure mechanism for skirted footing under static loading. However, the skirt length was limited to $0.6B$ only. In a few cases, earlier studies also observed the development of failure surfaces from the soil confined between skirts under static loading (Mana *et al.* 2012, Shukla and Jakka 2022).

3.2.2 Effect of footing depth ratio (D_f/B)

The influence of the depth ratio (D_f/B) on the seismic bearing capacity factor ($N_{\gamma q}$) and improvement (I_f) is highlighted by plotting the data and showing their variations with the same. As shown in Fig. 9, $N_{\gamma q}$ increases and I_f reduces with the increase in the D_f/B ratio. The increase in $N_{\gamma q}$ is attributed to increased confinement and increased surcharge above the foundation. The enhancement with footing depth is always greater under static loading than

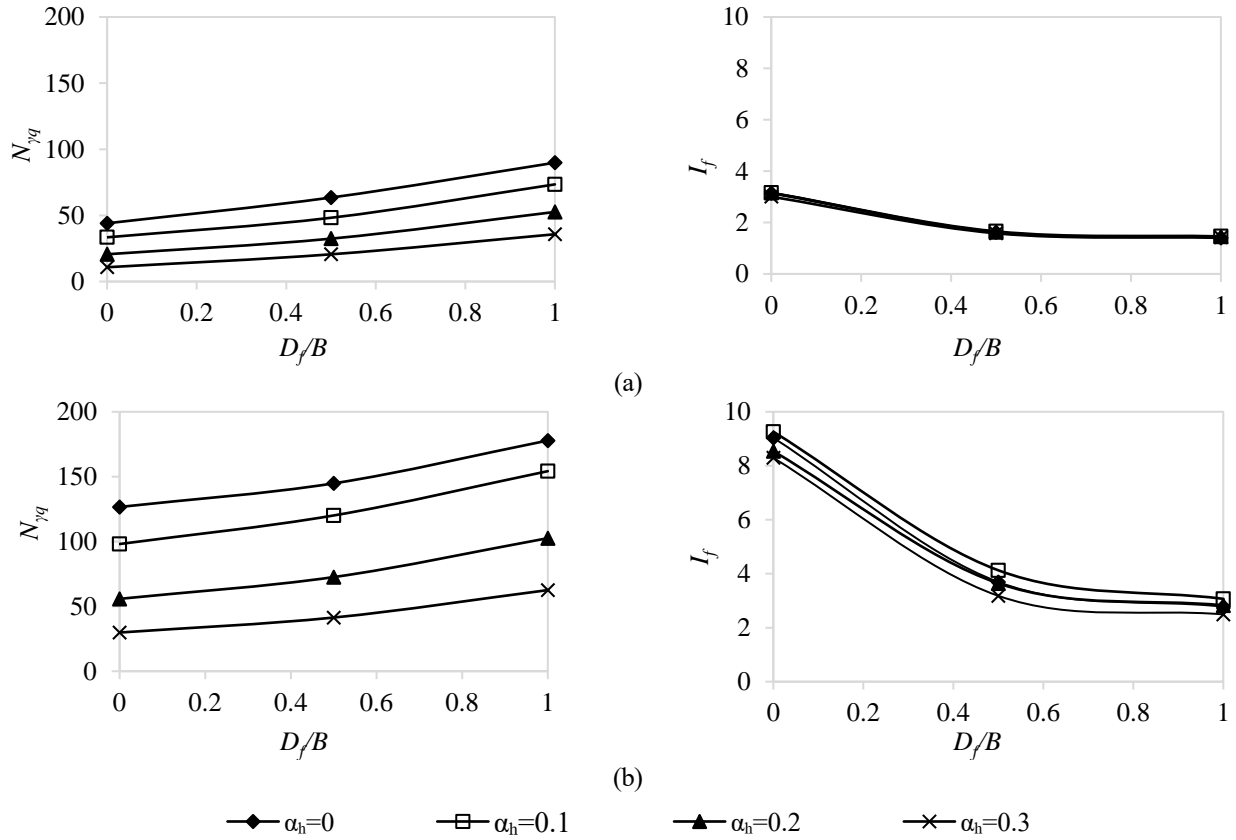


Fig. 9 Variation in $N_{\gamma q}$ and I_f with depth ratio: (a) $L/B=0.5$ and (b) $L/B=2$

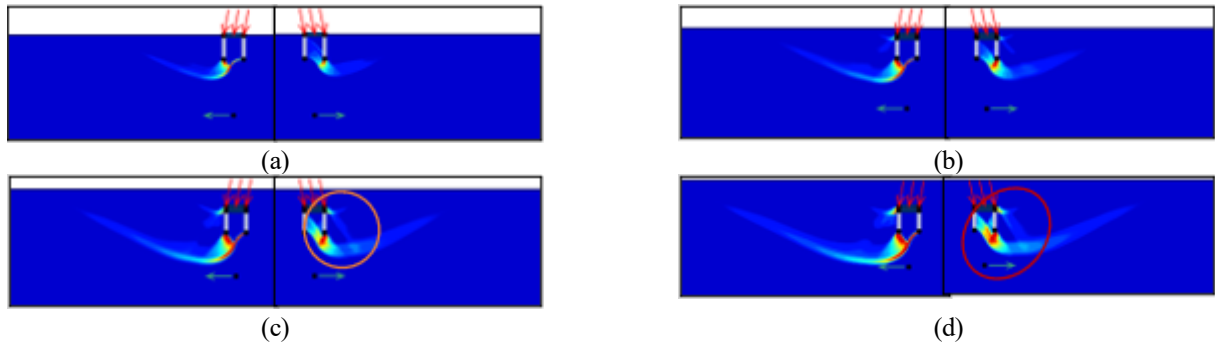


Fig. 10 Effect of embedment depth on failure mechanism: (a) $D_f/B=0$, (b) $D_f/B=0.5$, (c) $D_f/B=1.0$ and (d) $D_f/B=1.0$

seismic loading. The increase in $N_{\gamma q}$ with the D_f/B ratio diminishes with skirt length and seismic loading. The effectiveness of the skirt, as indicated by the improvement factor (I_f) reduces with footing depth (Figs. 9(a) and 9(b)). The confining effect enhances with the footing depth, but it reduces the improvement factor of the skirted footings as the skirt is more effective in soil with a low internal friction angle. The adverse impact of footing depth on the effectiveness of these foundations intensifies with an increase in skirt length. Seismic loading, which imposes horizontal forces, reduces the confining effect associated with increased footing depth; thus, the negative influence of footing depth is diminished under seismic loading conditions. This relationship is depicted in Figs. 9(a) and 9(b).

The effect of footing depth on the failure mechanism for rigid and deformable skirted footings of length $1.0B$ is shown in Fig. 10. The left and right parts in each Figure represent the shear dissipation plots for rigid and deformable skirts, respectively. The shear zone increases with embedment depth, thereby enhancing the seismic bearing capacity factor. The increase in footing depth in the area is substantial in rigid skirted footing compared to the deformable skirted footing. However, the failure mechanism is observed to be unaffected with increased footing depth. Figs. 9(a) and 9(b) depicts that the improvement factor (I_f) reduces with the increase in footing depth even though the shear zone area increases. This contrary behaviour is due to the increase in the bearing

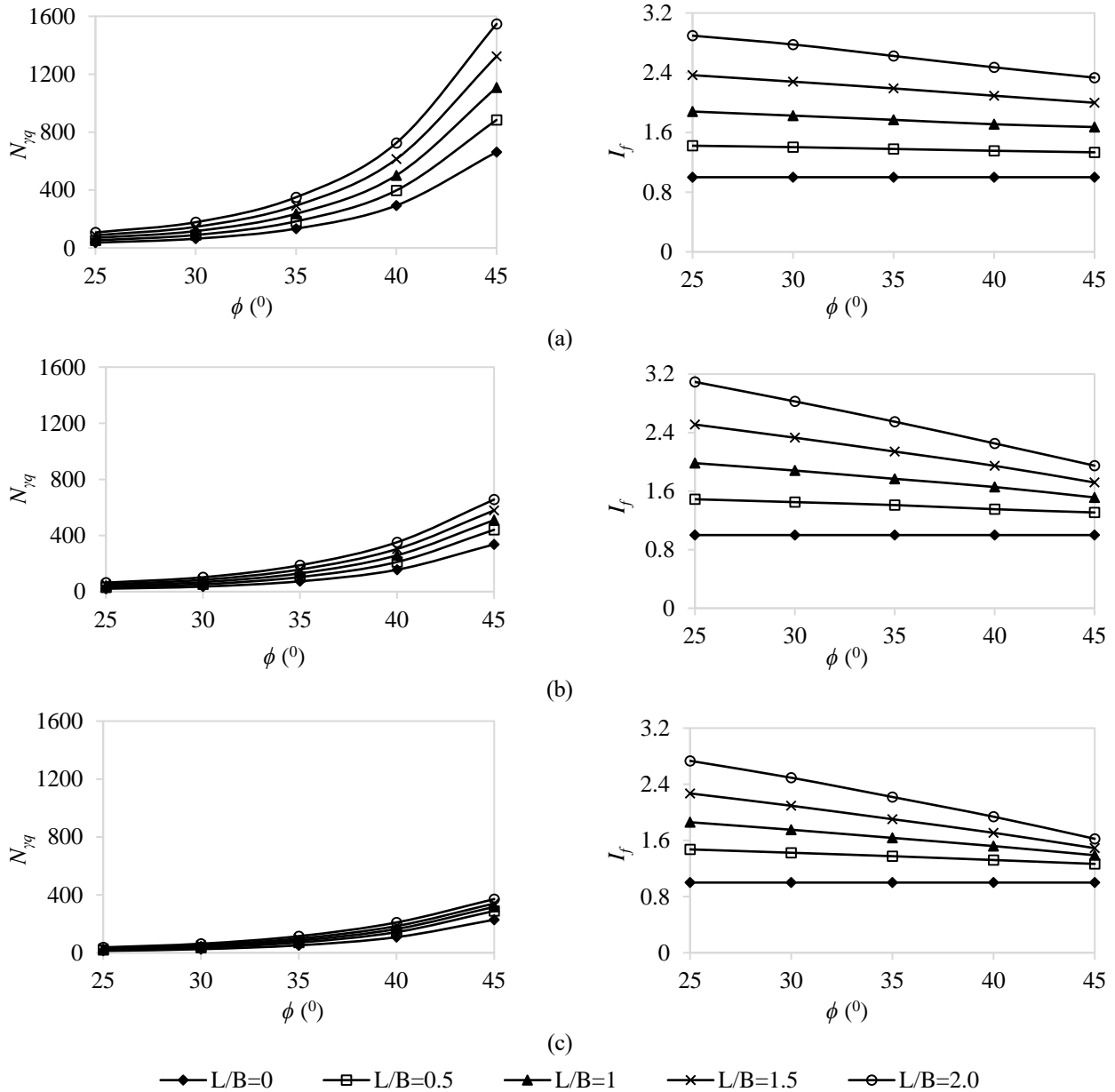


Fig. 11 Variation in $N_{\gamma q}$ and I_f with with angle of internal friction: (a) $\alpha_h=0.0$, (b) $\alpha_h=0.2$ and (c) $\alpha_h=0.3$

capacity (or shear zone area), with footing depth is comparatively very large in conventional strip footing than the skirted footing. The deflection of the deformable skirt increases with an increase in footing depth. It further reduced the effectiveness of the deformable skirt and skirted footing, which behaved identically to the conventional strip footing (highlighted in red). In a flexible skirted footing, when the skirt length exceeds the optimal value ($L/B > 1.5$), the failure surfaces begin inside the soil plug confined by the skirt, leading to minimal influence from the skirt. In contrast, for a rigid skirt, failure always starts at the tip of the skirt, regardless of its length, and an elastic region forms below the skirt tips. An elastic region develops for flexible skirts when the skirt length is less than $1.0B$, and the soil has a low friction angle. With larger skirts, however, the skirt experiences deflection, and an elastic zone forms at the

contact point between the skirt and the footing. The passive (plastic) region increases with the length of the rigid skirt.

However, the area of the passive region becomes almost constant for a skirt length greater than $1B$.

3.2.3 The effect of internal friction angle of soil (ϕ)

Fig. 11 show that the factors $N_{\gamma q}$ increase, and I_f decreases with the increase in the values of ϕ . The reduction in I_f increases with skirt length and seismic loading. The relative increase in shear strength and stiffness of loose soil is significant compared to dense soil. Therefore, I_f reduces with an increase in the ϕ . The reinforcing effect also increases with a reduction in the relative density of sand (Gray and Al-Refai 1986, Shukla 2017). The reinforcing effect induced by the skirt also reduces with the internal friction angle of the soil. These

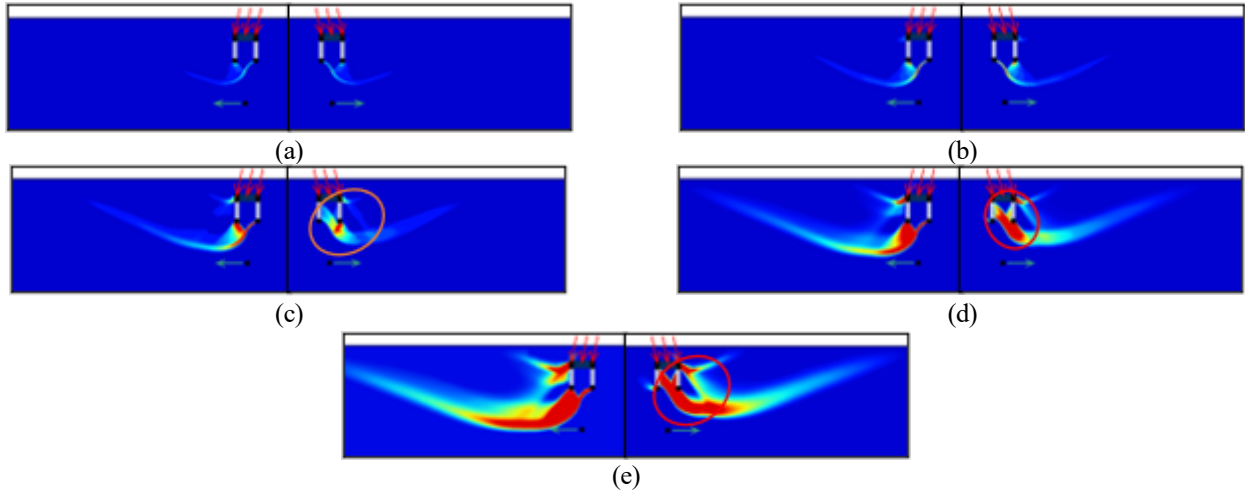


Fig. 12 The variation in failure mechanism with internal friction angle (a) $\phi=25^\circ$, (b) $\phi=30^\circ$, (c) $\phi=35^\circ$, (d) $\phi=40^\circ$ and (e) $\phi=45^\circ$

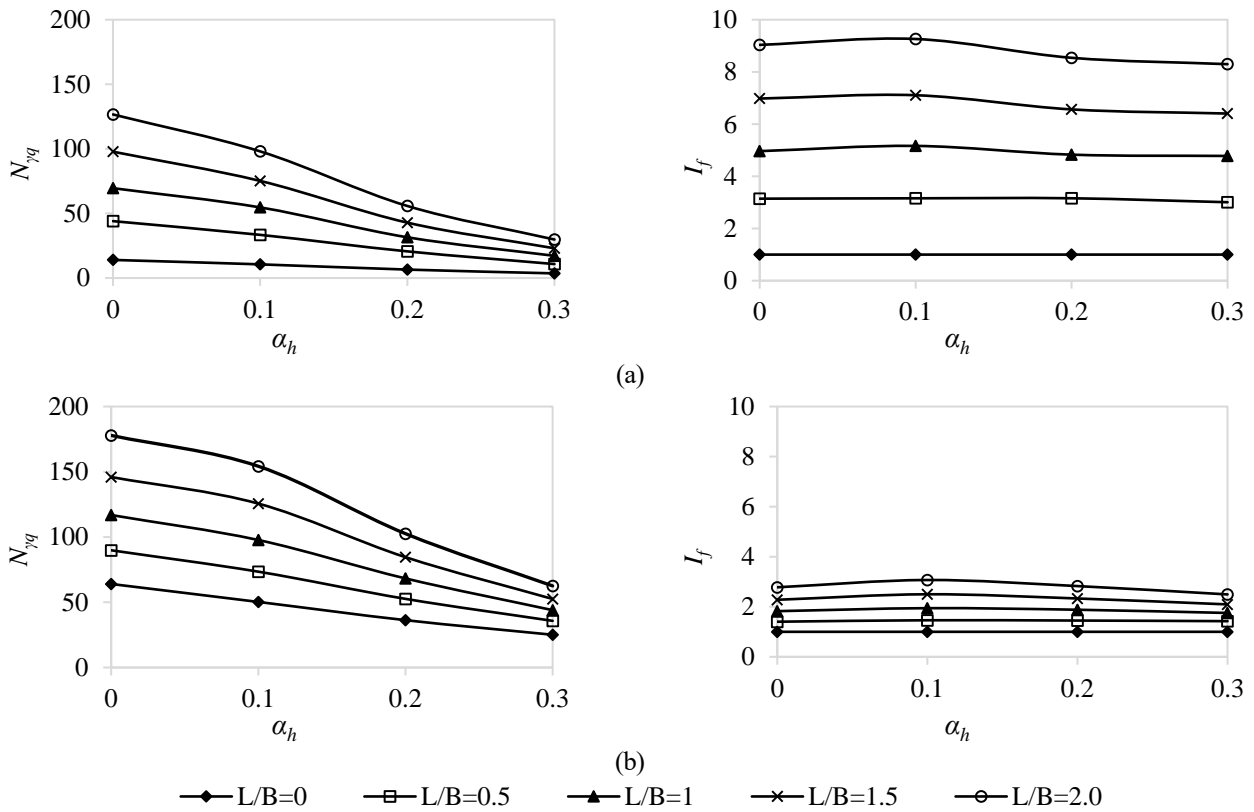


Fig. 13 Variation in $N_{\gamma q}$ and I_f with with seismic loading: (a) $D_f/B = 0$ and (b) $D_f/B = 1$

factors lead to a significant reduction in the skirt effectiveness with an internal friction angle. Both Eid (2013) and ElWakil (2013) also found that skirt effectiveness reduces with increased soil density.

Fig. 12 shows that the shear zone area increases with ϕ , which contributes to the increased bearing capacity. The enlargement in the shear zone is relatively higher in rigid skirted footing than in deformable skirted footing. The stiffness of the deformable skirt relative to soil decreases with the internal friction angle. Therefore, the skirt does not pose a restraint to the lateral displacement of soil and

deflects with soil toward the direction of soil displacement, which significantly reduces the skirt effectiveness. Deflection becomes more noticeable with an increase in internal friction angle, and footing behaves as traditional strip footing (Figs. 12(c), 12(d), 12(e)). The drawback of the deformable skirt can be lessened by replacing it with a rigid skirt, which does not deflect even in soils with a large internal friction angle (Figs. 12(a)-12(e)).

3.2.4 The effect of seismic acceleration (α_h)

The effects of the horizontal earthquake acceleration (α_h)

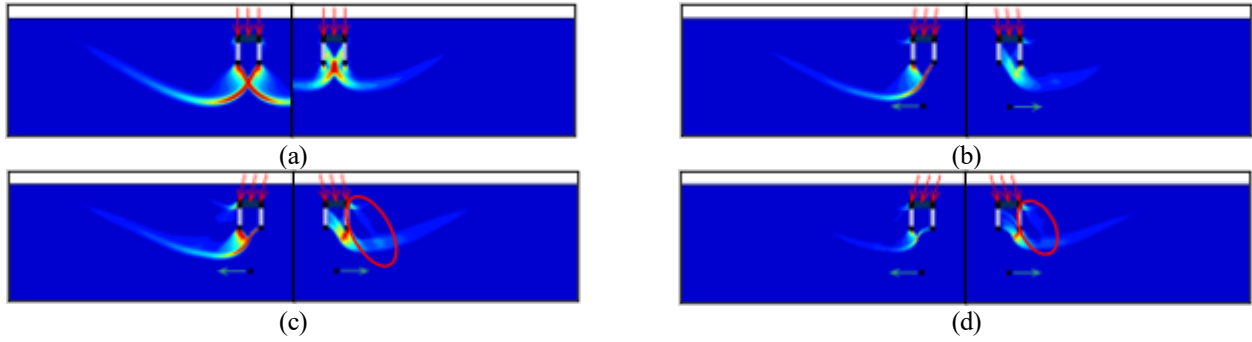


Fig. 14 Effect of seismic acceleration on skirted foundation failure mechanism (a) $\alpha_h=0$, (b) $\alpha_h=0.1$, (c) $\alpha_h = 0.2$ and (d) $\alpha_h=0.3$

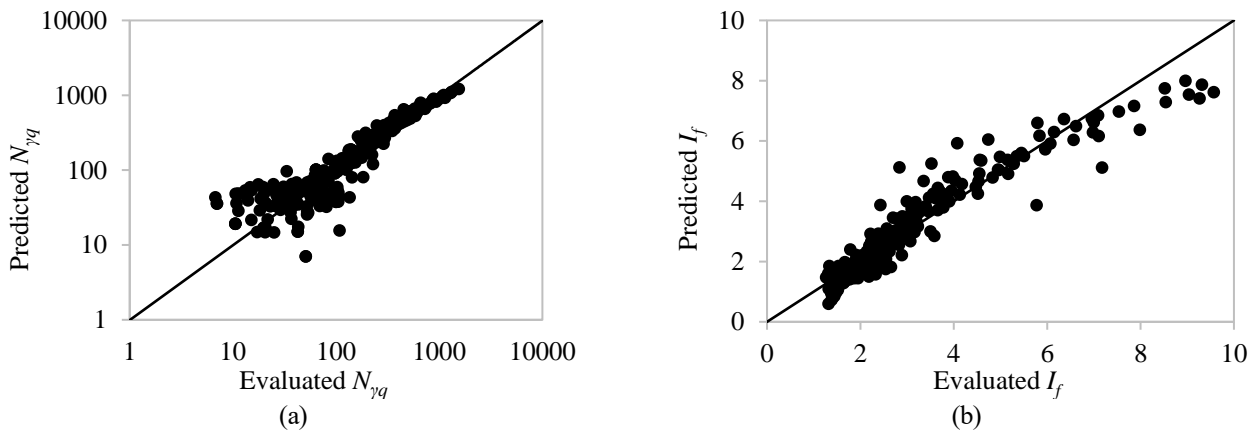


Fig. 15 Comparison of predicted values with determined value: (a) bearing capacity factor (b) improvement factor

on the bearing capacity factor and the influence factor are shown in Figs. 13. The bearing capacity factor reduces with increased seismic acceleration (horizontal pseudo-static coefficient). Contrary to the bearing capacity factor, the skirt effectiveness initially increases with the seismic acceleration of 0.1 g and decreases with further increases in seismic acceleration. This phenomenon becomes more observable with an increase in footing depth. A small increase in seismic acceleration reduces soil strength and stiffness, increasing effectiveness. However, a further increase in seismic loading decreases the combined stiffness of the soil-foundation system and induces excessive deformation. Therefore, the effectiveness of the skirt is also reduced. Figs. 13 shows that the influence of seismic loading on skirt effectiveness intensified with an increase in footing depth. The effects of seismic loading on the bearing capacity factor and its effectiveness increase with skirt length.

The effect of seismic acceleration (varying from 0 to 0.3) on the failure mechanism of skirted footing under seismic loading is shown in Fig. 14. The shear zone area is reduced by seismic loading, which reduces the bearing capacity reflected in the values of the bearing capacity factor. The failure surface is symmetrical for the static case ($\alpha_h=0$), and strength mobilization is equal on both sides of the footing axis. Only one side of strength is mobilized under seismic loading, and the failure surface becomes one-sided under seismic loading.

The deformable skirt deflects under seismic loading, and the deflection increases with an increase in the seismic loading, and the skirted footing behaves like a traditional strip footing (Figs. 14(c) and 14(d)). The slip surface originates from rigid skirt tips, and the elastic wedge forms below the skirts tip even at high seismic acceleration (Figs. 14(a)-14(d)).

In contrast, the slip surfaces originate from the connection point of the deformable skirt and footing. The failure mechanism is seen to change (from general shear failure to local shear failure) with the increase in seismic loading (Fig. 14(d)). Under a sizeable seismic acceleration, the influence of the deformable skirt becomes negligible and behaves identically to a strip footing. Based on the present study, it is suggested to use a rigidly skirted instead of a flexible skirt to get the optimal advantage of the skirt.

4. Statistical analysis

Statistical analysis of the obtained results was carried out to identify and assess the impact of the important and significant but independent parameters, namely, soil strength, skirt length, depth ratio and seismic acceleration (e.g. L/B , α_h , D_f/B , ϕ) on the enhancement of bearing capacity for rigid skirts. It was further found that the relationship between these parameters and the improvement factor and the independent variables is highly nonlinear for

rigid skirts. For quantitative estimation of the influence of the above parameters on the improvement factors and bearing capacity factors regression analysis was conducted, trying different types of equations through the data. Out of the different models (e.g., linear, exponential, logarithmic and polynomial logarithmic) that had been tried, the polynomial equation was found to provide the best prediction for the seismic bearing capacity and the corresponding improvement factor for rigid skirted footing.

The equations thus established to predict the bearing capacity factor and improvement are as presented by Eqs. (2) and (3). The terms in the predictive equations have been minimized as much as possible without significantly affecting the predictive accuracy.

$$N_{\gamma q} = 5.61 + 140 \tan \phi (2.5 - L/B - 1.78 D_f/B - 10 \tan \phi + 16 \alpha_h) + 350 \tan^2 \phi (L/B + 1.55 D_f/B + 4.428 \tan \phi - 12.85 \alpha_h) \quad (2)$$

$$I_f = 4 - 1.25 \alpha_h + 2.5 L/B + 2.1 \tan^2 \phi (\tan \phi - 2.67 + 2.24 D_f/B) + 2.6 D_f/B (1.27 D_f/B - \tan \phi L/B - 2.54) \quad (3)$$

where, B is width of footing in m; D_f = depth of footing in m; L = length of the skirt in m; I_f = improvement factor; $N_{\gamma q}$ = bearing capacity factor considering soil weight and surcharge together; α_h = horizontal pseudo-static coefficient ϕ = angle of internal friction of soil in degree
The coefficient of determination (R^2) is 0.94 for Eq. (2) and 0.91 for Eq. (3). The R^2 values greater than 0.90 indicate that the proposed predictive models demonstrate a strong fit to the data. Fig. 15 compares the predicted and evaluated bearing capacity factor and improvement factors. It demonstrates a high degree of agreement between the two sets of values. Notably, the minimum value of the improvement factor is 1.

5. Conclusions

From the studies presented above with regard to the seismic bearing capacity of skirted footings, the following conclusions are drawn.

The inclusion of a skirt enhances both seismic and static bearing capacities. However, the effectiveness of the skirt is influenced by multiple factors, including the stiffness of the skirted footing, skirt length, embedment ratio, and the internal friction angle of the soil. Overall, both the effectiveness of the skirt and bearing capacity improve with increased skirt length.

The bearing capacity of skirted footing decreases with seismic loading. The effectiveness of the rigid skirt (indicated by I_f) exhibits a nonlinear response to increasing seismic loading, where it initially improves but subsequently declines as the seismic intensity continues to rise. Similarly, the seismic bearing capacity rises, while the skirt effectiveness decreases with footing depth and internal friction of soil. The optimum skirt length varies between $0.5B$ to $1.5B$ in the flexible skirt. However, any length can be maintained in the case of a rigid skirt.

The flexible skirt shows 20%-50% less improvement than rigid skirted footing. The difference between rigid and skirted footing becomes more visible with an increase in the

seismic loading and angle of internal friction.

The failure mechanism shows that the rigid skirted footing behaves like a conventional strip footing placed at the tip level of the skirt. However, a deformable skirt with a longer skirt length deflects significantly and behaves differently from the rigid skirted footing. For deformable skirted footings, the elastic wedge does not develop for a skirt length greater than $1.5B$.

The failure pattern changes from general to local shear failure with increasing seismic acceleration and reduced internal friction angle. In the case of the longer rigid skirt, the confined failure is predominant. The failure mechanism remains unaffected despite increasing the footing depth. The failure mechanism also shows the difference in the effectiveness of rigid and deformable skirts, which augment with an increase in footing depth, skirt length, and internal friction angle of soil. Two equations that were developed yield good predictions for assessing the values of improvement factor and seismic bearing capacity of rigid skirted foundations.

References

- Al-Aghbari, M.Y. and Mohamedzein, Y.A. (2006), "Improving the performance of circular foundations using structural skirts", *Proceedings of the Institution of Civil Engineers-Ground Improvement*, **10**(3), 125-132. <https://doi.org/10.1680/grim.2006.10.3.125>.
- Al-Aghbari, M.Y. and Mohamedzein, Y.A. (2018), "The use of skirts to improve the performance of a footing in sand", *Int. J. Geotech. Eng.*, 1-8. <https://doi.org/10.1080/19386362.2018.1429702>.
- Al-Aghbari, M.Y. and Dutta, R.K. (2008), "Performance of square footing with structural skirt resting on sand", *Geomech. Geoeng.*, **3**(4), 271-277. <https://doi.org/10.1080/17486020802509393>.
- Al-Shyoukhi, T., Elmeligy, M. and Altahrany, A.I. (2023), "Experimental and numerical parametric studies on inclined skirted foundation resting on sand", *Civil Eng. J.*, **9**(7), 1795-1807. <https://doi.org/10.28991/CEJ-2023-09-07-017>.
- Azzam, W.R. (2015), "Finite element analysis of skirted foundation adjacent to sand slope under earthquake loading", *HBRC J.*, **11**(2), 231-239. <https://doi.org/10.1016/j.hbrcj.2014.04.001>.
- Azzam, W.R. and ElWakil, A.Z. (2015), "Experimental and numerical studies of circular footing resting on confined granular subgrade adjacent to slope", *Int. J. Geomech.*, [https://doi.org/10.1061/\(ASCE\)GM.1943-5622.0000500,04015028](https://doi.org/10.1061/(ASCE)GM.1943-5622.0000500,04015028).
- Bashir, K., Shukla, R. and Jakka, R.S. (2023), "Skirted footing for enhancing load-carrying capacity", *Proceedings of the Geo-Congress 2023*, 554-563. <https://doi.org/10.1061/9780784484685.056>.
- Bishop, A.W. (1966), "The strength of soils as engineering materials", *Geotechnique*, **16**(2), 91-130. <https://doi.org/10.1680/geot.1966.16.2.91>.
- Biswas, S. and Mittal, S. (2017), "Square footing on geocell reinforced cohesionless soils", *Geomech. Eng.*, **13**(4), 641-651. <https://doi.org/10.12989/gae.2017.13.4.641>.
- Bransby, M.F. and Yun, G.J. (2009), "The undrained capacity of skirted strip foundations under combined loading", *Geotechnique*, **59**(2), 115-125. <https://doi.org/10.1680/geot.2007.00098>.

- Bransby, M.F. and Randolph, M.F. (1999), "The effect of skirted foundation shape on response to combined V-M-H Loadings", *Int. J. Offshore Polar Eng.*, **9**(3), 214-218.
- Chakraborty, D. and Kumar, J. (2013), "Bearing capacity of foundations on slopes", *Geomech. Geoeng.*, **8**(4), 274-285.
- Chen, W.F. and Liu, X.L. (2012), Limit analysis in soil mechanics.
- Chen, W. and Randolph, M.F. (2007), "External radial stress changes and axial capacity for suction caissons in soft clay", *Géotechnique*, **57**(6), 499-511. <https://doi.org/10.1680/geot.2007.57.6.499>.
- Chetia N. and Saikia, B.D. (2015), "Improvement of bearing capacity of model footing with structural skirts on soft ground", *Proceedings of the 50th IGC*, 17-19 December 2015, Pune, Maharashtra, India.
- Demir, A. and Sarici, T. (2017), "Bearing capacity of footing supported by geogrid encased stone columns on soft soil", *Geomech. Eng.*, **12**(3), 417-439. <https://doi.org/10.12989/gae.2017.12.3.417>.
- Eid, H.T. (2013), "Bearing capacity and settlement of skirted shallow foundations on sand", *Int. J. Geomech.*, **13**(5), 645-652. [https://doi.org/10.1061/\(ASCE\)GM.1943-5622.0000237](https://doi.org/10.1061/(ASCE)GM.1943-5622.0000237).
- EL Wakil, A.Z. (2013), "Bearing capacity of skirt circular footing on sand", *Alexandria Eng. J.*, **52**, 359-364. <https://doi.org/10.1016/j.aej.2013.01.007>.
- Gray, D.H. and Al-Refeai, T. (1986), "Behavior of fabric vs. fiber-reinforced sand", *J. Geotech. Eng. ASCE*, **112**(8), 804-820. [https://doi.org/10.1061/\(ASCE\)0733-9410\(1986\)112:8\(804\)](https://doi.org/10.1061/(ASCE)0733-9410(1986)112:8(804)).
- Hu, Y., Randolph, M.F. and Watson, P.G. (1999), "Bearing response of skirted foundation on nonhomogeneous soil", *J. Geotech. Geoenviron. Eng.*, **125**(11), 924-935. [https://doi.org/10.1061/\(ASCE\)1090-0241\(1999\)125:11\(924\)](https://doi.org/10.1061/(ASCE)1090-0241(1999)125:11(924)).
- Huynh, Q.T., Lai, V.Q., Shiao, J., Keawsawasvong, S., Mase, L.Z. and Tra, H.T. (2022), "On the use of both diaphragm and secant pile walls for a basement upgrade project in Vietnam", *Innov. Infrastruct. Solut.*, **7**(1), 17. <https://doi.org/10.1007/s41062-021-00625-7>.
- Keawsawasvong, S. and Ukritchon, B. (2017), "Undrained stability of an active planar trapdoor in non-homogeneous clays with a linear increase of strength with depth", *Comput. Geotech.*, **81**, 284-293. <https://doi.org/10.1016/j.compgeo.2016.08.027>.
- Khatri, V.N., Debbarma, S.P., Dutta, R.K. and Mohanty, B. (2017), "Pressure-settlement behavior of square and rectangular skirted footings resting on sand", *Geomech. Eng.*, **12**(4), 689-705. <https://doi.org/10.12989/gae.2017.12.4.689>.
- Krabbenhöft, K., Lyamin, A.V. and Sloan, S.W. (2007), "Formulation and solution of some plasticity problems as conic programs", *Int. J. Solids Struct.*, **44**(5), 1533-1549. <https://doi.org/10.1016/j.ijsolstr.2006.06.036>.
- Kumar, J. (2003), "N_γ for rough strip footing using the method of characteristics", *Can. Geotech. J.*, **40**(3), 669-674. <https://doi.org/10.1139/t03-009>.
- Kumar, J. and Khatri, V. (2008), "Effect of footing roughness on lower bound N_γ values", *Int. J. Geomech. ASCE*, **8**(3), 176-187. [https://doi.org/10.1061/\(ASCE\)1532-3641\(2008\)8:3\(176\)](https://doi.org/10.1061/(ASCE)1532-3641(2008)8:3(176)).
- Lemaitre, J. (Ed.). (2001), Handbook of materials behavior models, three-volume set: Nonlinear models and properties.
- Lyamin, A.V., Salgado, R., Sloan, S.W. and Prezzi, M. (2007), "Two- and three-dimensional bearing capacity of footings in sand", *Géotechnique*, **57**(8), 647-662. <https://doi.org/10.1680/geot.2007.57.8.647>.
- Mana, D.S., Gourvenec, S.M., Randolph, M.F. and Hossain, M.S. (2012), "Failure mechanisms of skirted foundations in uplift and compression", *Int. J. Phys. Model. Geotech.*, **12**(2), 47-62. <https://doi.org/10.1680/ijpmg.11.00007>.
- Mana, D.S., Gourvenec, S.M., Randolph, M.F. and Hossain, M.S. (2012), "Failure mechanisms of skirted foundations in uplift and compression", *Int. J. Phys. Model. Geotech.*, **12**(2), 47-62. <https://doi.org/10.1680/ijpmg.11.00007>.
- Mana, D.S., Gourvenec, S. and Martin, C.M. (2013), "Critical skirt spacing for shallow foundations under general loading", *J. Geotech. Geoenviron. Eng.*, **139**(9), 1554-1566. [https://doi.org/10.1061/\(ASCE\)GT.1943-5606.0000882](https://doi.org/10.1061/(ASCE)GT.1943-5606.0000882).
- Mana, D.S., Gourvenec, S. and Randolph, M.F. (2014), "Numerical modelling of seepage beneath skirted foundations subjected to vertical uplift", *Comput. Geotech.*, **55**, 150-157. <https://doi.org/10.1016/j.compgeo.2013.08.007>.
- Martin, C.M. (2005), "Exact bearing capacity calculations using the method of characteristics", *Proc. IACMAG*, Turin, 441-450.
- Mase, L.Z., Putri, M.A., Edriani, A.F., Lai, V.Q. and Keawsawasvong, S. (2023), "Prediction of the bearing capacity of strip footing at the homogenous sandy slope based on the finite element method and multivariate adaptive regression spline", *Transport. Infrastruct. Geotechnol.*, 1-27. <https://doi.org/10.1007/s40515-023-00334-x>.
- Mase, L.Z., Saputra, J., Edriani, A.F. and Keawsawasvong, S. (2022), "Finite element analysis to estimate bearing capacity of strip footing in coastal sandy soils in Bengkulu City, Indonesia", *Eng. J.*, **26**(5), 59-75. <https://doi.org/10.4186/ej.2022.26.5.59>.
- Meyerhof, G.G. (1965), "Shallow foundations", *J. Soil Mech. Found. Eng. ASCE*, **91**(2), 21-31. <https://doi.org/10.1061/JSFEAQ.0000719>.
- Moradi, G., Abdolmaleki, A. and Soltani, P. (2019), "Small-and large-scale analysis of bearing capacity and load-settlement behavior of rock-soil slopes reinforced with geogrid-box method", *Geomech. Eng.*, **18**(3), 315-328. <https://doi.org/10.12989/gae.2019.18.3.315>.
- Nazir, A.K. and Azzam, W.R. (2010), "Improving the bearing capacity of footing on soft clay with sand pile with/without skirt", *Alexandria Eng. J.*, **49**, 371-377.
- Optum G2. Optum Computational Engineering, Copenhagen, Denmark.
- Randolph, M.F. and Watson, P.G. (1999), "Bearing response of skirted foundation on nonhomogeneous soil", *J. Geotech. Geoenviron. Eng. ASCE*, 924-934. [https://doi.org/10.1061/\(ASCE\)1090-0241\(1999\)125:11\(924\)](https://doi.org/10.1061/(ASCE)1090-0241(1999)125:11(924)).
- Saleh, N.M., Alsaied, A.E. and Elleboudy, A.M. (2008), "Behavior of skirted strip footing under eccentric load", *Proceedings of the 17th Int. Conf. on Soil Mechanics and Geotechnical Engineering*, 586-589.
- Shukla, R.P. and Jakka, R.S. (2022), "Bearing capacity and failure mechanism of skirted footings", *Geomech. Eng.*, **30**(1), 51-66. <https://doi.org/10.12989/gae.2022.30.1.051>.
- Shukla, R.P. and Jakka, R.S. (2023), "Failure mechanism and bearing capacity of inclined skirted footings", *Geomech. Eng.*, **35**(1), 41-54. <https://doi.org/10.12989/gae.2023.35.1.041>.
- Shukla, R.P. (2022), "Skirted footing subjected to inclined loading resting on cohesive soils", *Mag. Civil Eng.*, **108**(2), 1-14. <https://doi.org/10.34910/MCE.110.12>.
- Shukla, S.K. (2017). Fundamentals of Fibre-Reinforced Soil Engineering, Springer Nature Singapore Pld.
- Sloan, S.W. (2013), "Geotechnical stability analysis", *Géotechnique*, **63**(7), 531-571. <https://doi.org/10.1680/geot.12.RL.001>.
- Stergiou, T., Terzis, D. and Georgiadis, K. (2015), "Undrained bearing capacity of tripod skirted foundations under eccentric loading", *Geotechnik*, **38**(1), 17-27. <https://doi.org/10.1002/gete.201400029>.
- Tani, K. and Craig, W.H. (1995), "Bearing capacity of circular foundations on soft clay of strength increasing with depth", *Soils Found.*, **35**(4), 21-35. https://doi.org/10.3208/sandf.35.4_21.
- Terzaghi, K. (1943), Theoretical Soil Mechanics, Wiley, New York.

- Ukritchon, B., Whittle, A. and Klangvijit, C. (2003), "Calculations of bearing capacity factor N_γ using numerical limit analyses", *J. Geotech. Geoenviron. Eng.*, **129**(5), 468-474. [https://doi.org/10.1061/\(ASCE\)1090-0241\(2003\)129:6\(468\)](https://doi.org/10.1061/(ASCE)1090-0241(2003)129:6(468)).
- Vulpe, C. (2015), "Design method for the undrained capacity of skirted circular foundations under combined loading: Effect of deformable soil plug", *Géotechnique*, **65**(8), 669-683. <https://doi.org/10.1680/geot.14.P.200>.
- Yin, J.H., Wang, Y.J. and Selvadurai, A.P.S. (2001), "Influence of nonassociativity on the bearing capacity of a strip footing", *J. Geotech. Geoenviron. Eng.*, **127**(11), 985-989.
- Yun, G. and Bransby, M.F. (2007b), "The undrained vertical bearing capacity of skirted foundations", *Soils Found.*, **47**(3), 493-506. <https://doi.org/10.3208/sandf.47.493>.
- Zhang, P. and Ding, H. (2011), "Bearing capacity of the bucket spudcan foundation for offshore jack-up drilling platforms", *Petroleum Explor. Development*, **38**(2), 237-242. [https://doi.org/10.1016/S1876-3804\(11\)60029-3](https://doi.org/10.1016/S1876-3804(11)60029-3).
- Zhu, D. (2000), "The least upper-bound solutions for bearing capacity factor N_γ ", *Soils Found.*, **40**(1), 123-129. <https://doi.org/10.3208/sandf.40.123>.